DOE/NV/26383-LTR2007-04

Letter Report

Yucca Mountain Environmental Monitoring Systems Initiative

Air Quality Scoping Study for Sarcobatus Flat, Nevada

prepared by

Johann Engelbrecht, Ilias Kavouras, Dave Campbell,
Scott Campbell, Steven Kohl and David Shafer
Desert Research Institute
Nevada System of Higher Education

submitted to

Nevada Site Office
National Nuclear Security Administration
U.S. Department of Energy
Las Vegas, Nevada

April 2007

The work upon which this report is based was supported by the U.S. Department of Energy under Contract #DE-AC52-06NA26383.

CONTENTS

LIST OF FIGURES

LIST OF TABLES

INTRODUCTION

The Desert Research Institute (DRI) is performing a scoping study as part of the U.S. Department of Energy's Yucca Mountain Environmental Monitoring Systems Initiative (EMSI). The main objective is to obtain baseline air quality information for Yucca Mountain and an area surrounding the Nevada Test Site (NTS).

Air quality and meteorological monitoring and sampling equipment housed in a mobile trailer (shelter) is collecting data at seven sites outside the NTS, including Ash Meadows National Wildlife Refuge, Sarcobatus Flat, Beatty, Rachel, Caliente, Pahranagat National Wildlife Refuge, and Crater Flat, and at four sites on the NTS. The trailer is stationed at any one site for approximately eight weeks at a time.

Letter reports provide summaries of air quality and meteorological data, on completion of each site's sampling program.

SITE LOCATION AND CHARACTERISTICS

Sarcobatus Flat encompasses a dry lake bed, which covers approximately 30 square miles. It is part of the northern Amargosa Valley and the drainage of nearby Grapevine Mountains. It is about 30 miles north of Beatty and 40 to 50 miles northwest of the Yucca Mountain repository facility (Figure 1).

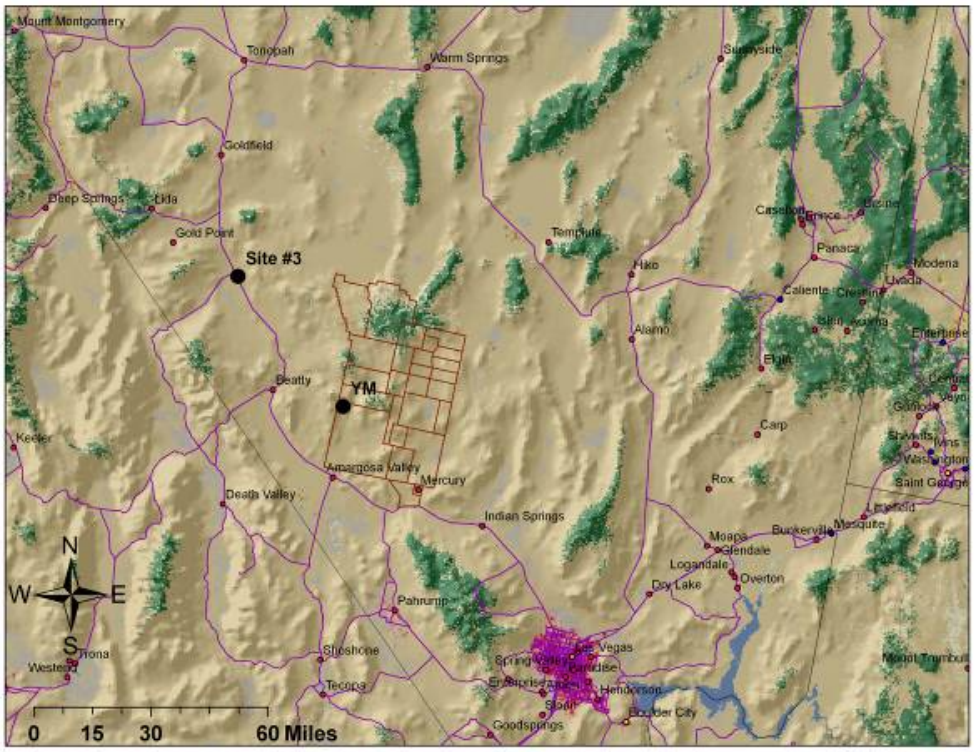

Figure 1. Southern Nevada map showing the location of Site #3 (at Sarcobatus Flat), Nevada Test Site, and Yucca Mountain. The map background is land use and land cover obtained from the 2001 National Land Cover Database.

The mobile trailer was located on private property about 3 miles south of the Scotty's Junction where Nevada State Route 267 meets with U.S. Highway 95. Location of the trailer is shown in Figure 2. Monitoring of PM_{10}, $PM_{2.5}$, and meteorological conditions was carried out from July 8, 2006, to September 6, 2006.

Table 1. Longitude, latitude, and elevation of the mobile trailer location at Site #3 (Sarcobatus Flat).

Site	Sarcobatus Flat
Latitude	37° 17' 10"
Longitude	117° 2' 4"

Figure 2. Location of the mobile trailer in Sarcobatus Flat. Image obtained from Google Earth.

AEROSOL SAMPLING AND MONITORING

Filter Sampling

Sampler Description and Procedures

BGI, Inc., PQ100 and PQ200 Ambient $PM_{2.5}$ Federal Reference Method (FRM) samplers were used to collect 24-h integrated PM_{10} and $PM_{2.5}$ samples. Figure 3 shows the PQ100 and PQ200 in the mobile trailer (left) and the PM_{10} sampling inlets on the top of the trailer (right). Both PQ100 (Designation No. RFPS-1298-124) and PQ200 (Designation No. RFPS-0498-116) are designed to meet the criteria for collecting 24-h samples of ambient aerosol according to the U.S. National Ambient Air Quality Standards (NAAQS).

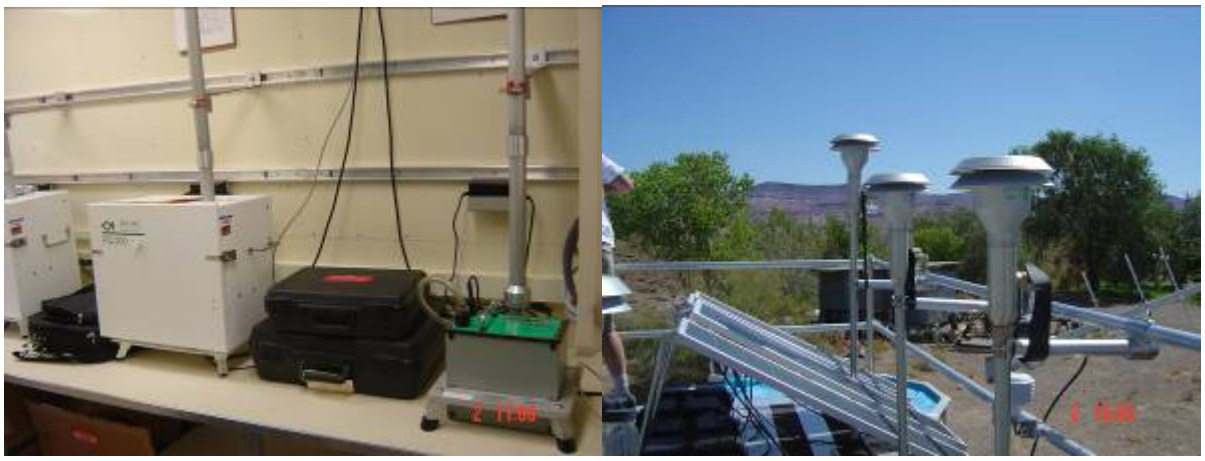

Figure 3. Photographs of PQ100 (green/gray box in left photo), PQ200 (white box in left photo) and their sampling inlet (right photo).

Figure 4 shows a schematic drawing of the samplers. Briefly, particles with aerodynamic diameter larger than 10 μm were removed by impaction at the size selective inlet, while the remaining particles remained airborne. For the PM_{10} fraction, particles were then collected by a filter located downstream of the size selective inlet. For the collection of $PM_{2.5}$, particles in the range between 2.5 and 10 μm were removed by the Very Sharp Cut Cyclone (VSCC) (U.S. Environmental Protection Agency [EPA] Equivalent Designation No. EQPM-0202-142), then collected by a filter.

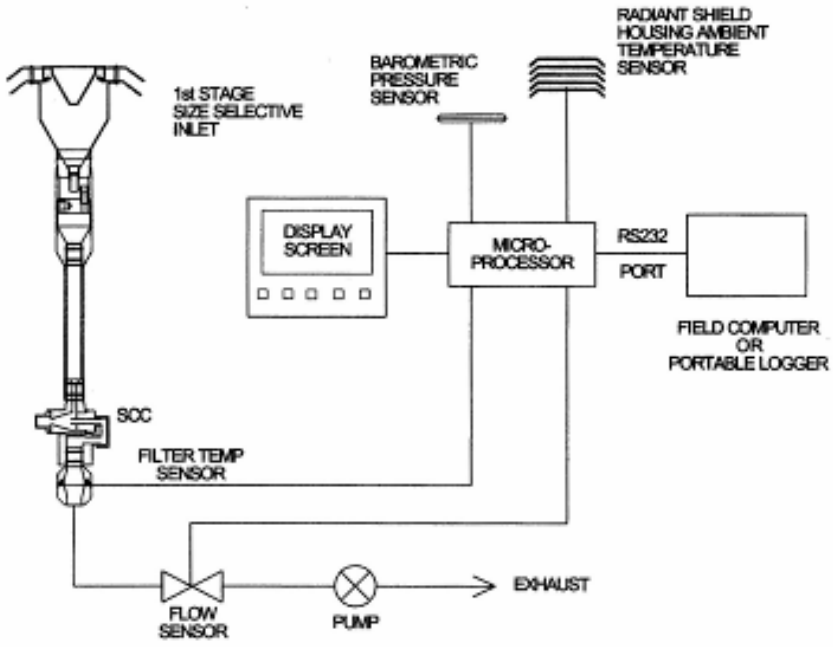

Figure 4. A diagrammatic representation of the BGI $PM_{2.5}$ sampler showing the PM_{10} size selective impactor head as the first stage followed by a $PM_{2.5}$ VSCC. This configuration can be readily modified to a PM_{10} sampler by removal of the VSCC.

For both PQ100 and PQ200, samples were collected at a volumetric flow rate of 16.67 liters/min. The flow rate is controlled to ±2 percent precision with a mass flow meter. The actual ambient temperature and barometric pressure, filter temperature and pressure, and anomalies (if any) were recorded (and controlled) by a microprocessor. The sampler was equipped to operate from an internal 12-volt DC battery. The battery was recharged by a battery charger from 120-volt AC. Alternatively, a 32-watt solar panel with an additional external ballast battery was installed to provide power for days without electricity. Two sets of PQ100 and PQ200 samplers were installed in the mobile trailer. PM_{10} and $PM_{2.5}$ samples were collected on filters in numbered cassettes, labeled TT (for PM_{10} Teflon), FT (for $PM_{2.5}$ Teflon), TQ (for PM_{10} Quartz), FQ (for $PM_{2.5}$ Quartz). Each filter cassette was loaded with a pre-weighed 46.2-mm-diameter PTFE (Teflon) membrane filter (Whatman # 7592-004) or 47-mm quartz fiber (Pallflex #2500QAT-UP) filter. The Teflon membrane collected particles for measurement of mass by gravimetric analysis, light absorption by densitometry, and elements by x-ray fluorescence spectrometry. Quartz fiber filters were used for measurement of water-soluble ions by atomic absorption spectrometry, ion chromatography, and automated colorimetry, and also for measurement of carbon species by thermal optical reflectance.

Operation, calibration, and maintenance of PQ100 and PQ200 are described in standard operation procedure (SOP) "BGI PQ100 PM10 and PQ200 PM2.5 REFERENCE SAMPLERS FOR THE YUCCA MOUNTAIN AIR QUALITY PROGRAM." Flow calibration and leak tests (only for PQ200) were performed on the day of installation (July 5, 2006). The leak check was performed according to the manufacturer's operational instruction manual only for PQ200; no procedure exists for the PQ100. The flow rate was calibrated using a BGI Tri-Cal flow meter. The sampler was then placed in calibration or "run" mode and a one-point calibration verification or one-point flow-rate verification was performed. Aerosol samples were collected on a 1-in-6-day schedule. Audits of the flow and leak tests were done onsite at the beginning and end of the monitoring campaign. Teflon and quartz filters were prepared and assembled in their filter holders in the Desert Research Institute's (DRI) Environmental Analysis Facility (EAF) in Reno and shipped to DRI's facilities in Las Vegas. The filters were kept at -4^{o}C and transported to the field in a cryo-cooler. Exposed filters were also stored at -4^{o}C in Las Vegas. Upon completion of the monitoring period at the site, all filters were shipped to the EAF in Reno.

Gravimetry

Table 2 shows mass concentrations (and uncertainty) of filters collected at Sarcobatus Flat. PM_{10} mass concentrations varied from 1.79 μg/m^3 to 8.78 μg/m^3, while $PM_{2.5}$ mass concentrations ranged from 1.91 μg/m^3 to 7.20 μg/m^3. Similar temporal trends were observed for both PM_{10} and $PM_{2.5}$. In all cases, 24-h PM_{10} and $PM_{2.5}$ levels were significantly lower than the daily and annual NAAQS as recently revised by EPA (24-h PM_{10}: 150 μg/m^3, 24-h $PM_{2.5}$: 35 μg/m^3; Annual $PM_{2.5}$: 15 μg/m^3) (Figure 5). Fine particles ($PM_{2.5}$) accounted for approximately two-thirds of PM_{10} ($PM_{2.5}/PM_{10}$ ratio of 0.60) (Figure 6). This value was comparable to that observed for traffic sites in urban areas probably due to the contribution of traffic emissions from U.S. Highway 95. However, note that PM_{10} and $PM_{2.5}$ concentration levels are quite low, which indicates the moderate-to-low contribution of windblown dust sources at Sarcobatus Flat for the monitoring period.

Table 2. Collection day, filter number, mass, and uncertainty determined by gravimetric analysis and associated flags of samples at Site #3 (Sarcobatus Flat).

Date	No	Type	Mass ($\mu g/m^3$)	Uncertainty ($\mu g/m^3$)	Flags
7/10/2006	026	PM_{10}	8.4443	0.5145	
		$PM_{2.5}$	4.3297	0.4940	
7/16/2006	027	PM_{10}	0.0000	0.4863	S: Suspect analysis result
		$PM_{2.5}$	4.7441	0.4953	
7/22/2006	028	PM_{10}	7.1131	0.5063	
		$PM_{2.5}$	3.9950	0.4927	
7/28/2006	029	PM_{10}	8.7770	0.5167	.
		$PM_{2.5}$	7.1993	0.5070	
8/03/2006	031	PM_{10}	5.8652	0.4999	
		$PM_{2.5}$	3.2057	0.4906	
8/09/2006	032	PM_{10}	1.7887	0.4873	
		$PM_{2.5}$	1.9143	0.4876	
8/15/2006	033	PM_{10}	7.1963	0.5068	
		$PM_{2.5}$	3.1640	0.4904	
8/21/2006	034	PM_{10}	5.5710	0.4986	
		$PM_{2.5}$	2.4563	0.4888	
8/27/2006	035	PM_{10}	7.9451	0.5113	
		$PM_{2.5}$	5.5764	0.4988	
9/02/2006	037	PM_{10}	6.9052	0.5052	
		$PM_{2.5}$	-99.0000	-99.0000	V: Invalid (void) analysis result

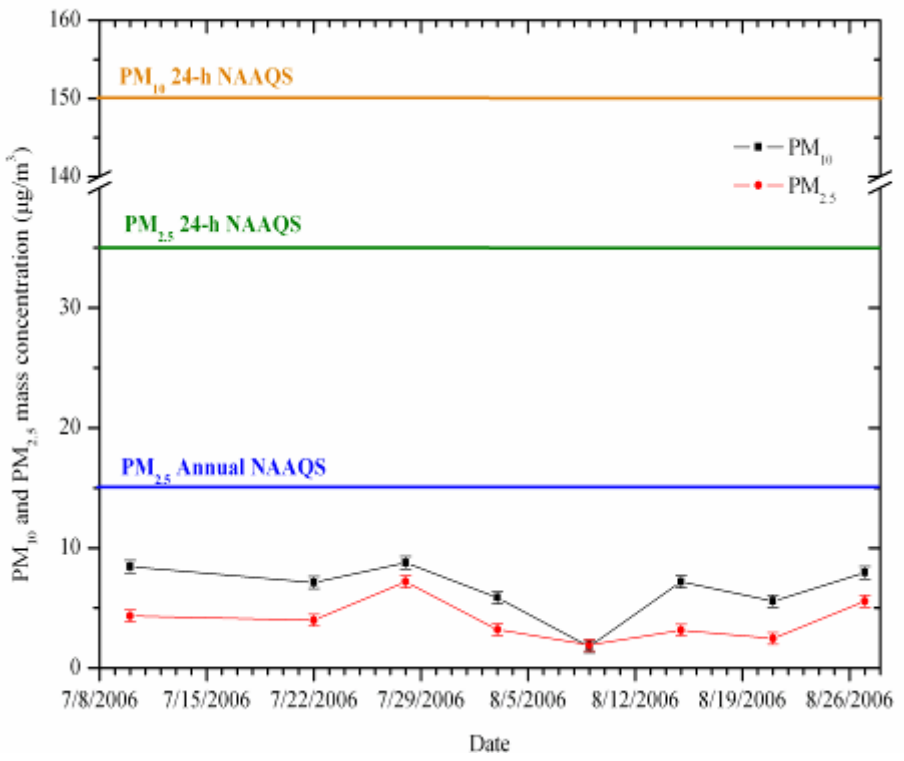

Figure 5. Time series of PM_{10} and $PM_{2.5}$ mass concentrations (mean ± uncertainty) at Site #3 (Sarcobatus Flat).

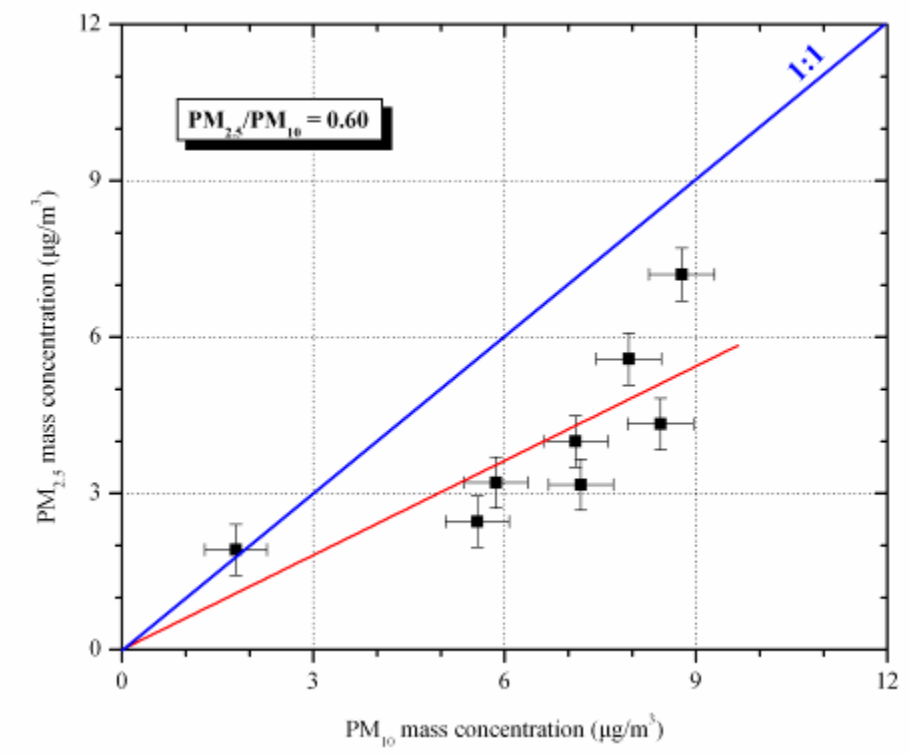

Figure 6. Relationship between mean (± uncertainty) daily $PM_{2.5}$ and PM_{10} at Sarcobatus Flat.

Chemical Analysis

Table 3 shows the chemical content of PM_{10} and $PM_{2.5}$ samples collected on 7/28/2006 and 8/15/2006. Chemical analysis included elements (from sodium to uranium) with x-ray fluorescence spectrometry, major anions (sulfate, nitrate, and chloride) by ion chromatography, major cations (sodium, potassium) by atomic absorption, particulate ammonium by colorimetry, and elemental and organic carbon by thermal optical reflectance (TOR).

Table 3. Results of the chemical analysis for selected filters from Sarcobatus Flat. Chemical components with concentration higher than two times the uncertainty are in bold, while those with concentrations lower than two times the uncertainty are in italics. Concentrations are in $\mu g/m^3$.

DATE	7/28/2006				8/15/2006			
SIZE	PM_{10}		$PM_{2.5}$		PM_{10}		$PM_{2.5}$	
	Conc.	Uncer.	Conc.	Uncer.	Conc.	Uncer.	Conc.	Uncer.
Chloride, Cl^-	*0.0513*	*0.0298*	*0.0055*	*0.0294*	*0.0167*	*0.0295*	*0.0067*	*0.0294*
Nitrate, NO_3^-	**0.3645**	**0.0303**	**0.0955**	**0.0295**	**0.3358**	**0.0302**	**0.1499**	**0.0296**
Sulfate, SO_4^{2-}	**1.365**	**0.0407**	**1.5234**	**0.043**	**0.5243**	**0.0313**	**0.5689**	**0.0317**
Ammonium, NH_4^+	**0.4545**	**0.0342**	**0.5206**	**0.0355**	**0.1801**	**0.0303**	**0.2054**	**0.0306**

Table 3. Results of the chemical analysis for selected filters from Sarcobatus Flat. Chemical components with concentration higher than two times the uncertainty are in bold, while those with concentrations lower than two times the uncertainty are in italics. Concentrations are in μg/m^3 (continued).

DATE	7/28/2006				8/15/2006			
SIZE	PM_{10}		$PM_{2.5}$		PM_{10}		$PM_{2.5}$	
	Conc.	Uncer.	Conc.	Uncer.	Conc.	Uncer.	Conc.	Uncer.
Sodium, Na^+	**0.1645**	**0.0039**	**0.0866**	**0.0025**	**0.1016**	**0.0028**	**0.0621**	**0.0022**
Potassium, K^+	**0.0973**	**0.0054**	**0.0743**	**0.0046**	**0.0453**	**0.0037**	**0.0237**	**0.0032**
OC1	**1.6512**	**0.2552**	**1.6804**	**0.2596**	**1.047**	**0.1626**	**1.4761**	**0.2283**
OC2	**1.3211**	**0.2542**	**1.2883**	**0.2482**	**0.7154**	**0.1451**	**0.9039**	**0.1787**
OC3	**0.9187**	**0.1976**	**0.9221**	**0.198**	**0.4663**	**0.17**	**0.495**	**0.1715**
OC4	**0.4979**	**0.1383**	**0.4469**	**0.1261**	**0.2718**	**0.0867**	**0.2265**	**0.0775**
Pyrolyzed OC-TT	**0.6795**	**0.1416**	**0.4584**	**0.0993**	**0.4257**	**0.0933**	**0.3191**	**0.0741**
Pyrolyzed OC-Op	**0.6242**	**0.122**	**0.3951**	**0.0824**	**0.1211**	**0.0434**	**0.2507**	**0.0596**
Total OC	**5.0107**	**0.59**	**4.7306**	**0.5617**	**2.6193**	**0.3573**	**3.3498**	**0.4255**
EC1	**0.7203**	**0.1488**	**0.5503**	**0.1151**	**0.3099**	**0.0688**	**0.3191**	**0.0705**
EC2	**0.165**	**0.0454**	**0.1128**	**0.0401**	**0.1158**	**0.0403**	**0.0987**	**0.0389**
EC3	**0**	**0.0116**	**0**	**0.0116**	**0**	**0.0116**	**0**	**0.0116**
Total EC	**0.2611**	**0.0953**	**0.268**	**0.0972**	**0.3046**	**0.1079**	**0.167**	**0.0697**
Total Carbon	**5.2719**	**0.4106**	**4.9986**	**0.3959**	**2.9239**	**0.2934**	**3.5169**	**0.3205**
Sodium, Na	*0.0515*	*0.15*	*0.0726*	*0.1504*	*0.0524*	*0.1501*	*0.0863*	*0.1507*
Magnesium, Mg	*0.1214*	*0.0452*	*0.0719*	*0.0449*	*0.0616*	*0.0448*	*0.0106*	*0.0446*
Aluminum, Al	**0.284**	**0.0196**	**0.1101**	**0.0182**	**0.2782**	**0.0195**	**0.0538**	**0.018**
Silicon, Si	**0.632**	**0.0209**	**0.2361**	**0.0157**	**0.5825**	**0.0201**	**0.1303**	**0.0148**
Phosphorous, P	**0.0183**	**0.0046**	*0.031*	*0.0046*	*0.0119*	*0.0045*	*0.0129*	*0.0046*
Sulfur, S	**0.4217**	**0.0221**	**0.6239**	**0.0242**	**0.2321**	**0.0208**	**0.247**	**0.0209**
Chlorine, Cl	**0.0149**	**0.0037**	*0.0011*	*0.0037*	*0.0011*	*0.0037*	*0*	*0.0037*
Potassium, K	**0.149**	**0.0036**	**0.1118**	**0.003**	**0.123**	**0.0032**	**0.0436**	**0.0021**
Calcium, Ca	**0.1911**	**0.0049**	**0.0706**	**0.0032**	**0.171**	**0.0045**	**0.0422**	**0.0029**
Scandium, Sc	*0*	*0.0074*	*0*	*0.0074*	*0*	*0.0074*	*0*	*0.0074*
Titanium, Ti	*0.017*	*0.0013*	**0.0067**	**0.0013**	**0.0194**	**0.0014**	**0.0047**	**0.0013**
Vanadium, V	*0*	*0.0003*	*0*	*0.0003*	*0*	*0.0003*	*0.0002*	*0.0003*
Chromium, Cr	*0*	*0.0015*	*0*	*0.0015*	*0*	*0.0015*	*0*	*0.0015*
Manganese, Mn	*0.0052*	*0.0032*	*0.0008*	*0.0032*	*0.0038*	*0.0032*	*0.0013*	*0.0032*
Iron, Fe	**0.1913**	**0.0051**	**0.0678**	**0.0035**	**0.1996**	**0.0053**	**0.0433**	**0.0034**
Cobalt, Co	*0*	*0.0003*	*0*	*0.0003*	*0*	*0.0003*	*0*	*0.0003*
Nickel, Ni	*0.0005*	*0.0008*	*0*	*0.0008*	*0*	*0.0008*	*0*	*0.0008*
Copper, Cu	*0.0003*	*0.0017*	*0*	*0.0017*	*0.0018*	*0.0017*	*0*	*0.0017*
Zinc, Zn	*0.0015*	*0.0015*	*0.001*	*0.0015*	*0.0005*	*0.0015*	*0*	*0.0015*
Gallium, Ga	*0*	*0.0049*	*0.0025*	*0.0049*	*0*	*0.0049*	*0.0015*	*0.0049*
Arsenic, As	*0*	*0.0006*	*0*	*0.0006*	*0*	*0.0006*	*0*	*0.0006*
Selenium, Se	*0*	*0.0011*	*0*	*0.0011*	*0*	*0.0011*	*0*	*0.0011*
Bromine, Br	*0.0023*	*0.0021*	*0.0038*	*0.0021*	*0*	*0.0021*	*0.0023*	*0.0021*
Rubidium, Rh	*0.0002*	*0.0011*	*0*	*0.001*	*0*	*0.001*	*0*	*0.001*
Strontium, Sr	**0.0054**	**0.0025**	*0.0029*	*0.0025*	*0.001*	*0.0025*	*0.0015*	*0.0025*
Yttrium, Y	*0.0011*	*0.0015*	*0.0002*	*0.0015*	*0.0011*	*0.0015*	*0*	*0.0015*
Zirconium, Zr	*0.0003*	*0.0039*	*0*	*0.0039*	*0*	*0.0039*	*0.0018*	*0.0039*
Niobium, Nb	*0*	*0.0025*	*0*	*0.0025*	*0*	*0.0025*	*0.0002*	*0.0025*

Table 3. Results of the chemical analysis for selected filters from Sarcobatus Flat. Chemical components with concentration higher than two times the uncertainty are in bold, while those with concentrations lower than two times the uncertainty are in italics. Concentrations are in μg/m^3 (continued).

DATE	7/28/2006				8/15/2006			
SIZE	PM_{10}		$PM_{2.5}$		PM_{10}		$PM_{2.5}$	
	Conc.	Uncer.	Conc.	Uncer.	Conc.	Uncer.	Conc.	Uncer.
Molybdenum, Mo	*0.0008*	*0.0025*	*0.0003*	*0.0025*	*0*	*0.0025*	*0*	*0.0025*
Palladium, Pd	*0*	*0.0059*	*0*	*0.0059*	*0*	*0.0059*	*0*	*0.0059*
Silver, Ag	*0*	*0.0056*	*0.0007*	*0.0056*	*0.0041*	*0.0056*	*0*	*0.0056*
Cadmium, Cd	*0*	*0.0044*	*0*	*0.0044*	*0.0013*	*0.0044*	*0*	*0.0044*
Indium, In	*0*	*0.0048*	*0*	*0.0048*	*0.0013*	*0.0049*	*0*	*0.0049*
Tin, Sn	*0*	*0.0053*	*0*	*0.0053*	*0*	*0.0053*	*0.0023*	*0.0053*
Antimony, Sb	*0.0026*	*0.008*	*0.0041*	*0.008*	*0.0011*	*0.008*	*0.0065*	*0.008*
Cesium, Cs	*0*	*0.0023*	*0*	*0.0023*	*0*	*0.0023*	*0*	*0.0023*
Barium, Ba	*0*	*0.0025*	*0.0002*	*0.0025*	*0*	*0.0025*	*0*	*0.0025*
Lanthanum, La	*0*	*0.0017*	*0*	*0.0017*	*0*	*0.0017*	*0.0008*	*0.0017*
Cerium, Ce	*0.0003*	*0.0016*	*0*	*0.0016*	*0.0008*	*0.0016*	*0*	*0.0016*
Samarium, Sa	*0*	*0.0033*	*0*	*0.0033*	*0.0005*	*0.0033*	*0*	*0.0033*
Europium, Eu	*0.0029*	*0.0051*	*0.0025*	*0.0051*	*0.0005*	*0.0051*	*0*	*0.0051*
Terbium, Tb	*0.0005*	*0.0037*	*0.0015*	*0.0037*	*0*	*0.0037*	*0*	*0.0037*
Hafnium, Hf	*0*	*0.0152*	*0*	*0.0152*	*0*	*0.0152*	*0*	*0.0151*
Tantalum, Ta	*0.0039*	*0.01*	*0*	*0.0099*	*0.0025*	*0.01*	*0.0034*	*0.01*
Tungsten, W	*0.0098*	*0.0164*	*0*	*0.0163*	*0*	*0.0164*	*0*	*0.0163*
Iridium, Ir	*0*	*0.0046*	*0*	*0.0046*	*0*	*0.0046*	*0.0015*	*0.0046*
Gold, Au	*0*	*0.0075*	*0*	*0.0075*	*0*	*0.0075*	*0*	*0.0075*
Mercury, Hg	*0.0003*	*0.0037*	*0.0018*	*0.0037*	*0*	*0.0037*	*0*	*0.0037*
Thallium, Th	*0*	*0.0025*	*0*	*0.0025*	*0*	*0.0025*	*0*	*0.0025*
Lead, Pb	*0*	*0.0036*	*0*	*0.0036*	*0.0013*	*0.0036*	*0*	*0.0036*
Uranium, U	*0*	*0.0063*	*0*	*0.0063*	*0.0041*	*0.0063*	*0*	*0.0063*

OC = organic carbon
EC = elemental carbon
OP = optical pyrolysis
TT = transmittance

With respect to the chemical composition of PM_{10} and $PM_{2.5}$, the following patterns are observed:

- Sulfur (S) was mostly in the form of sulfate (SO_4^{2-}) with sulfate-to-sulfur ratio of 2.25 to 3.23. Sulfate and ammonium were almost entirely (100% for sulfate, 100% for ammonium) associated with fine particles, while less than 50 percent of nitrate (26 to 45%) was measured in $PM_{2.5}$. Ammonium-to-sulfate molar ratios varied from 1.78 to 1.92, suggesting that sulfate aerosols were mostly in the form of ammonium bisulfate, $(NH_4)HSO_4$ (Malm *et al.*, 2002). Nitrates appeared to be partially neutralized by ammonium in the fine particle mode, while coarse particles nitrates may be the product of the reactions of nitric acid with soil dust elements such as Ca (Lefer and Talbot, 2001).
- Carbonaceous aerosol was predominantly in fine particles. For $PM_{2.5}$, organic carbon (OC) concentrations accounted for 69 to 111 percent of particle mass. This may be

attributed to the positive bias of OC concentrations caused by absorption of low vapor pressure organic compounds on the quartz filter. Overestimation also may explain the relatively low EC/OC ratio values (between 0.05 and 0.12), which were lower than those determined for atmospheric aerosol.

- Soluble potassium (K^+) accounted for 36 to 65 percent of total potassium in PM_{10} and for more than 50 percent of total potassium in $PM_{2.5}$. Soluble potassium is a tracer of biomass burning, which suggested the significant impact of emissions from local and/or regional fire (prescribed or wildfire) events. This was further supported by the estimates of nonsoil potassium $K_{non\text{-}soil}$ (K_{total}-(0.26 x [Al])) that were comparable to measured water-soluble K^+.
- Ratios of Al/Si (0.41 to 0.48) K/Fe (0.61 to1.64) were comparable to those determined for samples collected at the Interagency Monitoring of Protected Visibility Environments (IMPROVE) sites in western United States (Al/Si: 0.31 to 0.43, K/Fe: 0.67 to 0.78, Al/Ca: 1.4 to 1.7) when soil dust was the major component of particulate matter (Kavouras *et al*., 2006).

The IMPROVE mass estimation scheme is adopted to reconstruct aerosol mass into five major types: sulfate, nitrate, organic, light-absorbing carbon, and soil. For this scheme, sulfate and nitrate are assumed to be in the forms of ammonium sulfate [$(NH_4)_2SO_4$] and ammonium nitrate [NH_4NO_3], respectively (Malm *et al*., 2004). Organic mass concentration [OMC] was estimated as [OMC] =1.4 x [OC], where [OC] is the organic carbon concentration. The 1.4 factor was used to correct for other elements (mainly hydrogen and oxygen) associated with the composition of organic compounds (White and Roberts, 1977). Soil mass concentration [SOIL] was estimated as the sum of the elements present in the soil as oxides (Al_2O_3, SiO_2, CaO, K_2O, FeO, Fe_2O_3, and TiO_2) as follows:
[SOIL] = 2.2 x [Al] + 2.49 [Si] + 1.63 x [Ca] + 2.42 x [Fe] + 1.94 x [Ti]. Therefore, the reconstructed aerosol mass was estimated as follows:

$$[\text{Aerosol Mass}] = (128/96) \times [SO_4] + (80/62) \times [NO_3] + EC + [OMC] + [SOIL]$$

Figure 7 shows the concentrations of ammonium sulfate, ammonium nitrate, organic carbon mass, elemental carbon and soil for PM_{10} and $PM_{2.5}$ collected on 7/28/2006 and 8/15/2006 in Sarcobatus Flat. Considering the positive bias for organic carbon measurements:

- Reconstructed particle mass accounted for 111 to 144 percent of measured PM_{10} mass and for 142 to 204 percent of $PM_{2.5}$ mass.
- Carbonaceous aerosol (OMC and EC) appeared to account for 50 to 58 percent of PM_{10} and 67 to 75 percent of $PM_{2.5}$.
- Soil represented 24 to 36 percent of PM_{10} and about 10 percent of $PM_{2.5}$ mass, while sulfate contributed between 9 and15 percent on PM_{10} and 12 to 24 percent on $PM_{2.5}$ (Figure 7).
- The differences of PM_{10} and $PM_{2.5}$ fractions are due to higher concentration of soil elements in the coarse fraction (particles with diameter between 2.5 and 10 μm). Higher $PM_{2.5}$ mass concentrations for July 28, 2006, may be attributed to increased

concentrations of organic carbon and to a lesser extent on soil and sulfate concentrations.

- 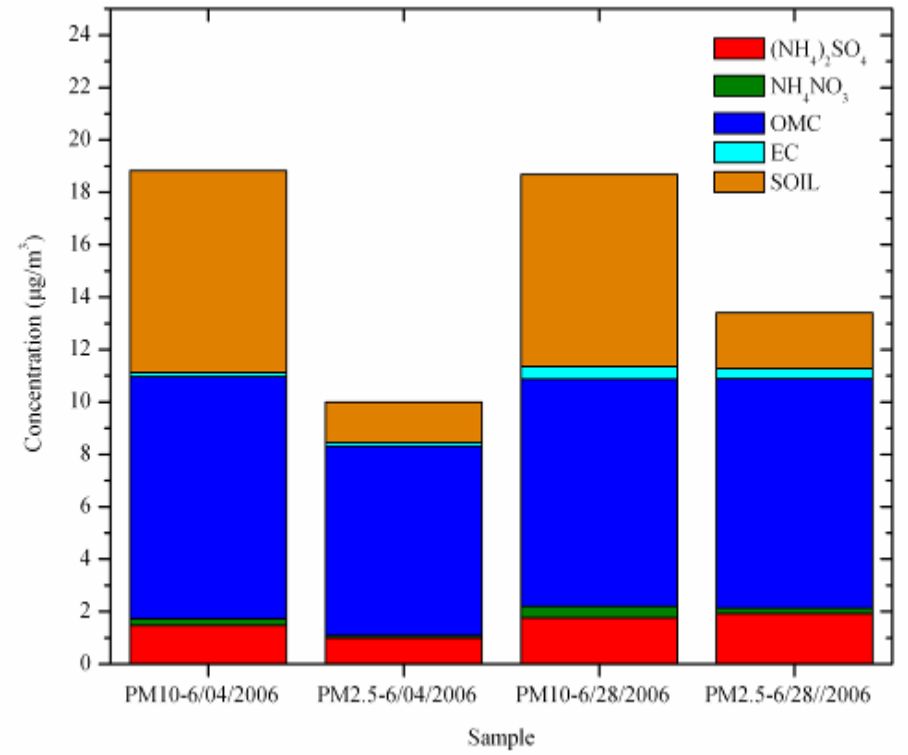

Figure 7. Reconstructed mass for PM_{10} and $PM_{2.5}$ based on chemical composition.

Aerosol Monitoring

Monitor Description and Procedures

The TEOM Series 1400 Ambient Particulate Monitor from Thermo Scientific and the DUSTTRAK™ Aerosol Monitor from TSI were used to continuously measure PM_{10} and $PM_{2.5}$ mass concentrations (Figure 8). The TEOM Series 1400 monitors the ambient particulate mass concentration of PM_{10} (EPA certification EQPM-1090-079) (or $PM_{2.5}$) in real time by direct measurement of particulate mass collected on a filter attached to an oscillating inertial mass transducer. The mass transducer in the sensor unit has a tapered ceramic tube (element) that is fixed at the downstream end and a Teflon-coated glass fiber filter on the free end. The oscillating frequency of the tube changes proportionally as ambient air is drawn through the filter and the particulate loading thereon increases. The flow-rate through the filter sample is set at a nominal 3.0 l/min. A bypass (auxiliary) flow provides an additional 13.67 l/min for a total flow-rate of 16.67 l/min. An internal datalogger stores mass values, time, and some meteorological data. To eliminate bias caused by humidity, the filter is heated to 50°C. Operation, calibration and maintenance of the TEOM is described in SOP "RUPPRECHT & PATASHNICK (R&P), SERIES 1400A TAPERED ELEMENT OSCILLATING MICROBALANCE (TEOM)." Flow calibration and leak tests were performed on the day of installation (March 24, 2007). Data were downloaded during site

visits. Regular checks of time, filter loading, by-pass filter, and flow rates were accomplished during site visits.

Figure 8. Left photograph: The front panels of PM_{10} (right on the left photograph) and $PM_{2.5}$ (left on the left photograph) of TEOM. Right photograph: The measurement units of TEOM and DUSTTRAK on top of them.

The DUSTTRAK™ Aerosol Monitor is a portable, battery operated laser photometer. The monitor provides measurements of particle mass based on 90^{o} light scattering. Atmospheric aerosol passes through a size selective inlet (either PM_{10} or $PM_{2.5}$) and is directed to an optics chamber at a flow rate of 1.7 l/min. The light source is a laser diode that emits light at a wavelength of 780 nm. The aerosol sample is drawn into the sensing chamber where it is illuminated with a narrow beam of laser light. Light scattered by aerosol particles is collected by a set of lenses and focused onto the photodetector. The detector signal is proportional to the amount of scattered light, which is proportional to the mass concentration of the aerosol. Voltage is read by the processor and multiplied by an internal calibration constant to yield mass concentration. The calibration constant is pre-set by the manufacturer for scattering characteristics of the respirable mass of ISO 12103-1, Al test dust. Local variations in aerosol particle size distribution and composition relative to this standard may result in differences in the actual response factor of the instrument. The operation, calibration, and maintenance of TSI is described in SOP "TSI INCORPORATED MODEL 8520 DUSTTRAK AEROSOL MONITOR FOR THE YUCCA MOUNTAIN AIR QUALITY PROGRAM."

Both PM_{10} and $PM_{2.5}$ DUSTTRAK inlets were attached on a wide "Y" connector, which was connected to one end of a second "Y' (Figure 9). A funnel was connected to the other end of the second "Y" to achieve fast exchange of ambient air into the sampling line. Flow calibration and zero-test were performed on the day of installation (July 5, 2006) and subsequent site visits. Deviations in flow were predominantly due to failure of the pump diaphragm. In those cases, the instrument was replaced. Deviations of the zero check were corrected by performing zero calibration according to the manufacturer's operational instruction manual.

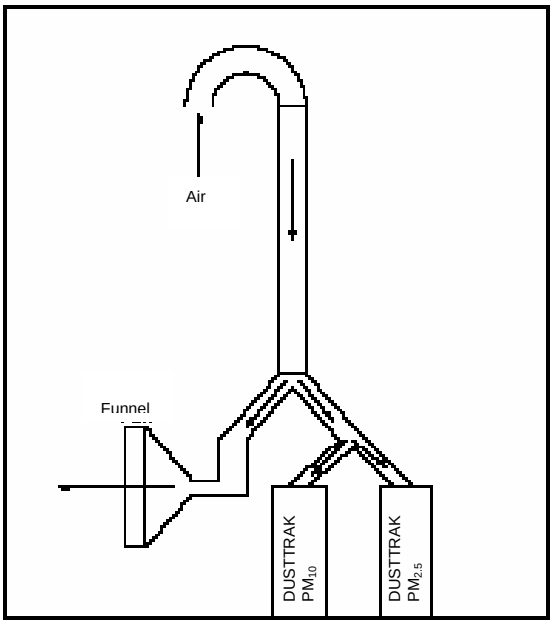

Figure 9. Sampling inlet for DUSTTRAK.

Continuous Measurements of PM_{10} and $PM_{2.5}$

Trends and correlations of particle mass are examined using hourly TEOM data integrated for 24 hours (from 0:00. to 23:00). Statistics of 24-h particle mass are presented in Table 4.

Table 4. Statistics for 24-h PM_{10} and $PM_{2.5}$ TEOM mass concentrations.

	Mean	Median	Minimum	Maximum	Std. Deviation
PM_{10}	14.8	13.9	8.0	42.8	5.6
$PM_{2.5}$	3.5	3.4	1.1	9.8	1.7

Twenty-four-h PM_{10} levels ranged from 8.0 to 42.8 $\mu g/m^3$, with a mean of 14.8 (σ=5.6) $\mu g/m^3$, while $PM_{2.5}$ concentrations varied from 1.1 to 9.8 $\mu g/m^3$, with a mean of 3.5 (σ=1.7) $\mu g/m^3$. Similar temporal trends were found for PM_{10} and $PM_{2.5}$ at Sarcobatus Flat. A high PM_{10} episode on August 10, 2006, was observed, with $PM_{2.5}$ mass concentration of approximately 9 $\mu g/m^3$ (Figure 10). A consistent relationship between PM fractions was observed during the monitoring period, with fine particles being accounted for about one-fourth of PM_{10} ($PM_{2.5}/PM_{10}$ ratio of 0.24) (Figure 11). While differences in particle mass for weekdays/weekends were not statistically significant, somewhat higher PM_{10} levels were measured on Thursday (Day #4) (Figure 12).

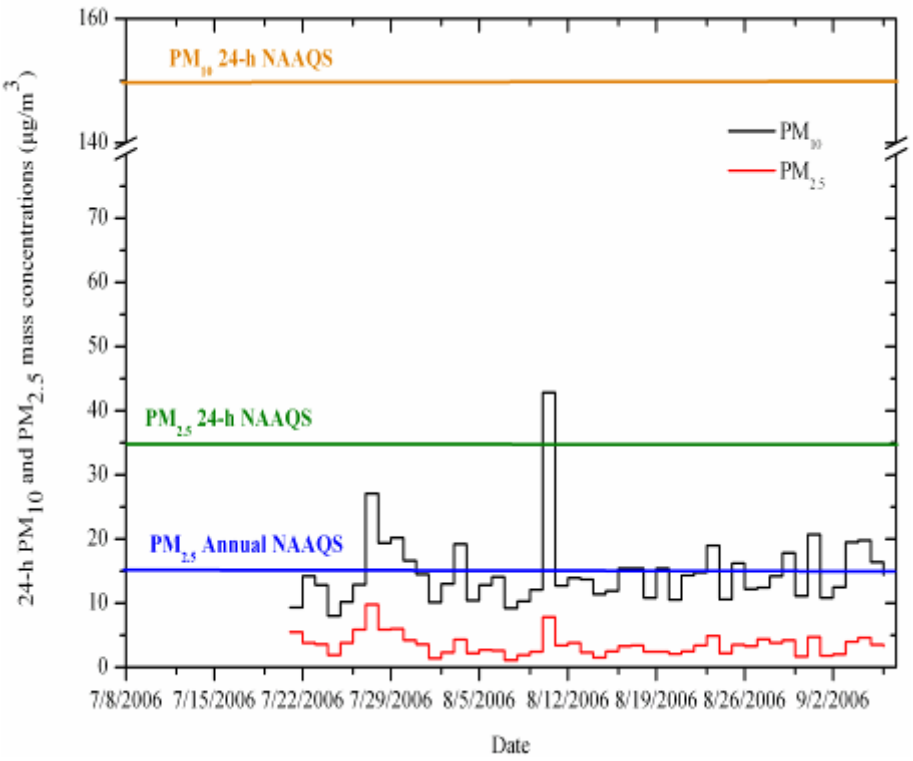

Figure 10. Mean 24-h PM_{10} and $PM_{2.5}$ mass concentrations measured by TEOM at Site #3 (Sarcobatus Flat).

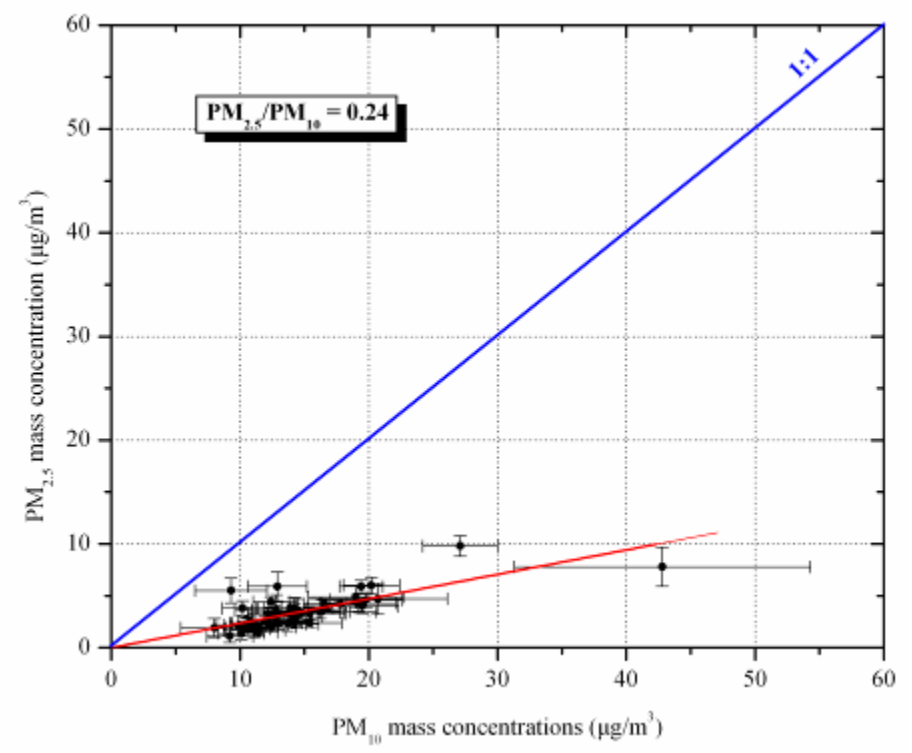

Figure 11. $PM_{2.5}/PM_{10}$ mass ratios at Site #3 (Sarcobatus Flat). Error bars represent the standard error of the mean.

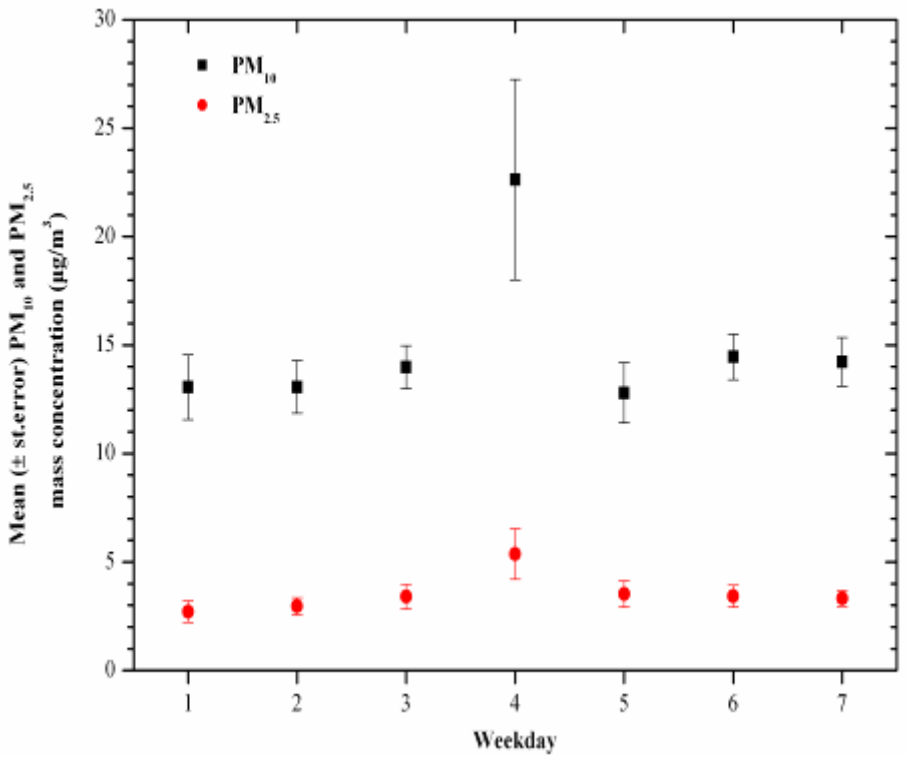

Figure 12. Variation of mean (± st.error) PM_{10} and $PM_{2.5}$ (µg/m^3) in weekdays and weekends at Site #3 (Sarcobatus Flat) (Monday=1, Tuesday=2, Wednesday=3, Thursday=4, Friday=5, Saturday=6, Sunday=7).

Variations of daily PM_{10} and $PM_{2.5}$ measured with DUSTTRAK and TEOM are presented in Figure 13 and Figure 14. The absolute differences between concentrations measured by DUSTTRAK and TEOM were larger for PM_{10} as compared to those for $PM_{2.5}$. Daily trends of particle mass concentrations measured by DUSTTRAK and TEOM were comparable for $PM_{2.5}$ mass. The time series plots for PM_{10} particle mass concentrations measured by TEOM and DUSTTRAK are somewhat comparable in shape and almost identical for $PM_{2.5}$. The temporal correlations between DUSTTRAK and TEOM were low to moderate (R=0.32 to 0.70). A slope of 0.20828 and an intercept of 1.82809 µg/m^3 (Figure 15) were computed for PM_{10}. This was indicative of the weakness of the light scattering technique to monitor dust particles that represented more than 70 percent of PM_{10} mass in Sarcobatus Flat at very low concentration levels. As for $PM_{2.5}$, both TEOM and DUSTTRAK were quite comparable, the slope between TEOM and DUSTTRAK $PM_{2.5}$ was 1.09189 with a rather low intercept of 0.56249 µg/m^3. This good agreement was due to the fact that light scattering provides more reliable measurements of particle mass in the accumulation mode.

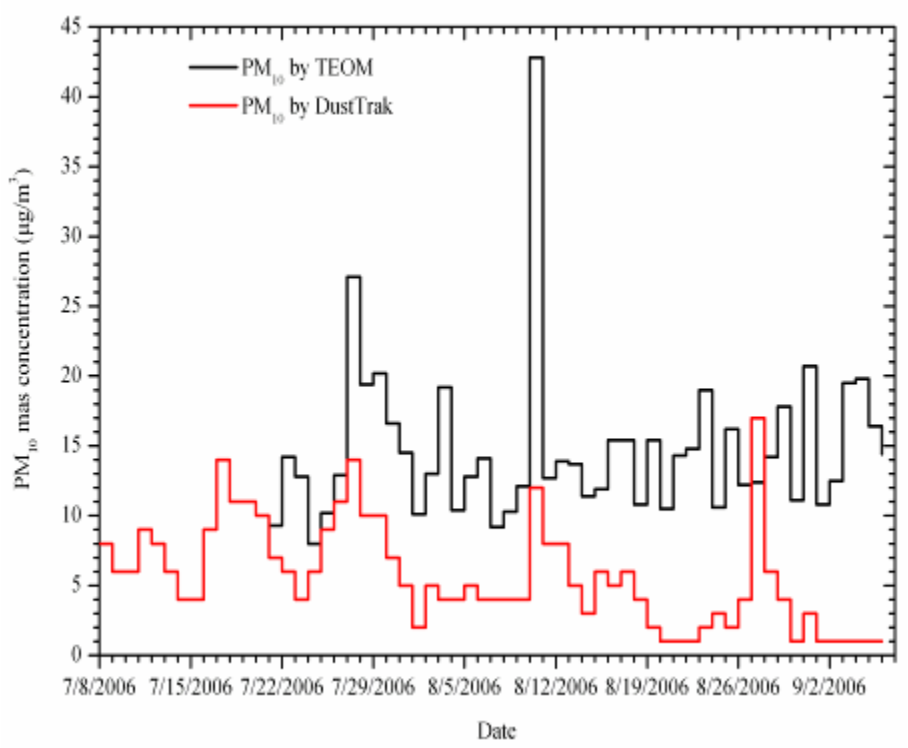

Figure 13. PM_{10} mass (µg/m^3) measured with DUSTTRAK and TEOM at Site #3 (Sarcobatus Flat).

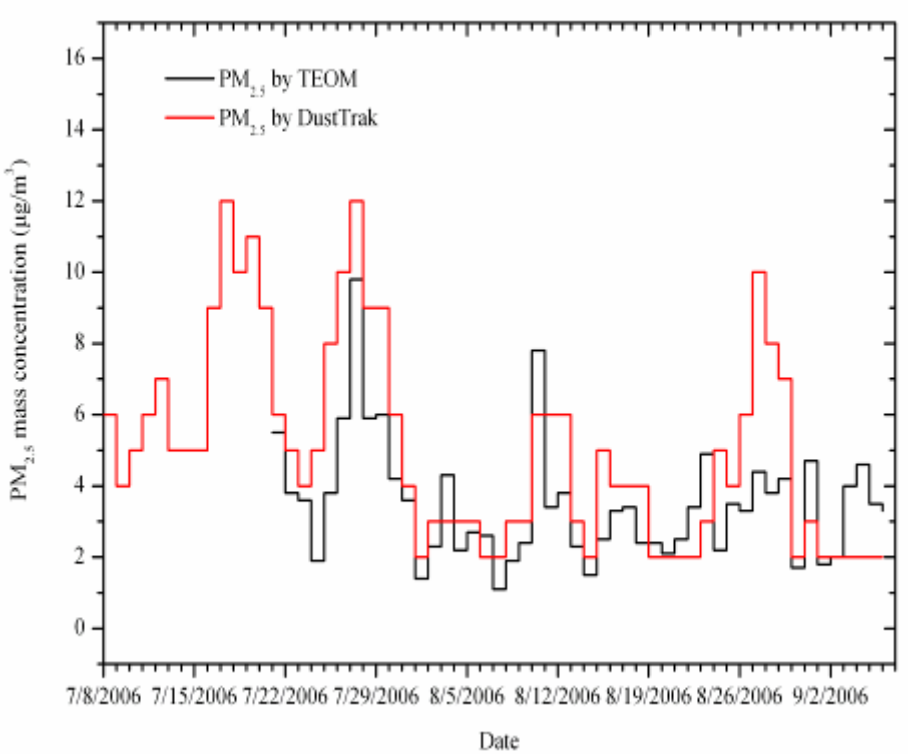

Figure 14. $PM_{2.5}$ mass (µg/m^3) measured with DUSTTRAK and TEOM at Site #3 (Sarcobatus Flat).

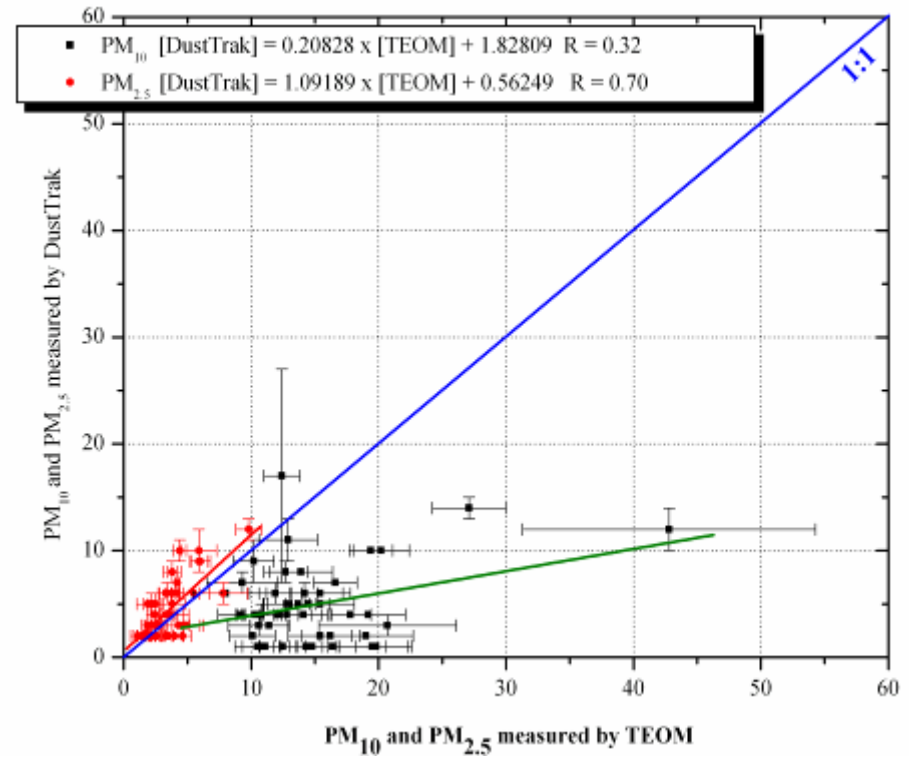

Figure 15. Comparison of 24-h PM_{10} and $PM_{2.5}$ mass concentrations measured by TEOM and DUSTTRAK. Error bars represent the standard error of the mean.

Comparison of Filter to Continuous Results

Figure 16 and Figure 17 show the relationships between PM_{10} and $PM_{2.5}$ measured by TEOM/DUSTTRAK and FRM filter-based methods. The temporal correlations between PM_{10} and $PM_{2.5}$ measurements by TEOM, DUSTTRAK, and filter methods were good, with correlation coefficients from 0.89 to 0.90. The slopes for $PM_{2.5}$ measured by TEOM and DUSTTRAK were 0.63728 and 1.488031, respectively, with insignificant intercepts. The agreement between TEOM/DUSTTRAK and filter-based PM_{10} measurements was quite poor (R=0.33 to 0.50), with slope of 0.47796 for TEOM and 1.12909 for DUSTTRAK, while high intercepts are computed. The poor correlation for PM_{10} may be attributed to the low range of filter-based values (10 to 20 $\mu g/m^3$; six valid samples).

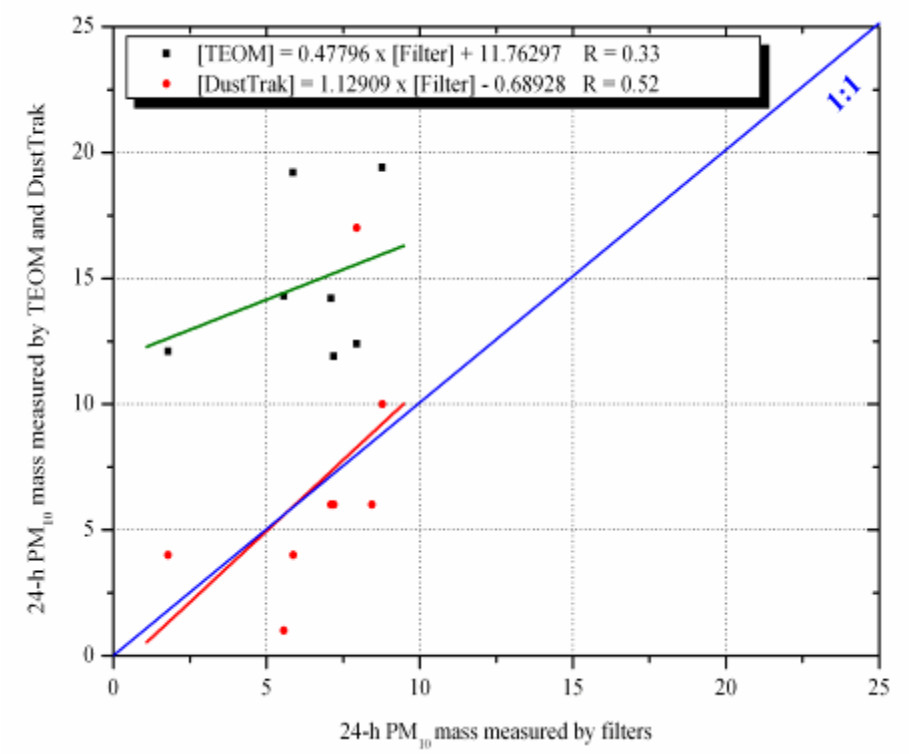

Figure 16. Relationships between PM_{10} concentrations (µg/m^3) measured by TEOM, DUSTTRAK, and filter-based methods.

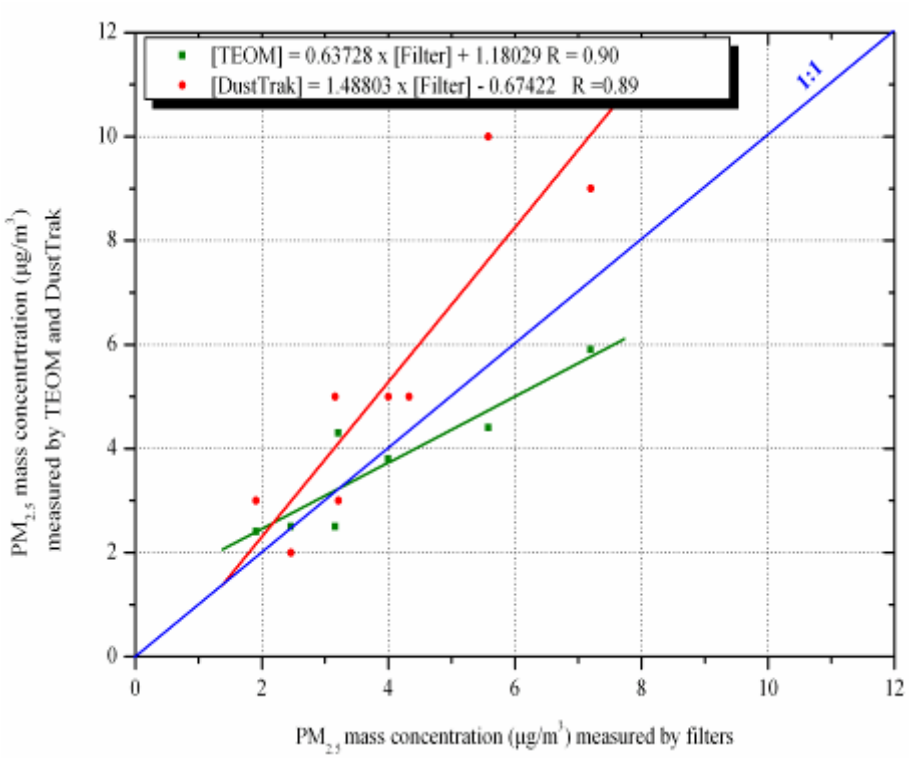

Figure 17. Relationships between $PM_{2.5}$ concentrations (µg/m^3) measured by TEOM, DUSTTRAK, and filter-based methods.

METEOROLOGY

Variations of hourly data for each meteorological parameter are presented in Figure 18 through Figure 22. Descriptive statistics of hourly data also are presented in Table 5. Solar radiation progressively increased up to 86.6 watts/m^2 (Figure 18). Ambient temperature varied from 48.7 to 106.9ºF with a mean temperature of 80.7ºF for the monitoring period (Table 5; Figure 19). Relative humidity remained lower than 30 percent except the last 10 days of July and at the end of the monitoring period, due to rainfall of 13.7 mm during these periods (Figure 20).

Table 5. Descriptive statistics of 1-hour meteorological data.

	Mean	Minimum	Maximum	Sum
Solar Radiation (watts/m^2)	25.4	0.0	86.6	
Wind speed (miles/h)	7.2	0.5	22.6	
Temperature (ºF)	80.7	48.7	106.9	
Relative humidity (%)	20	3	84	
Precipitation (mm)				13.71

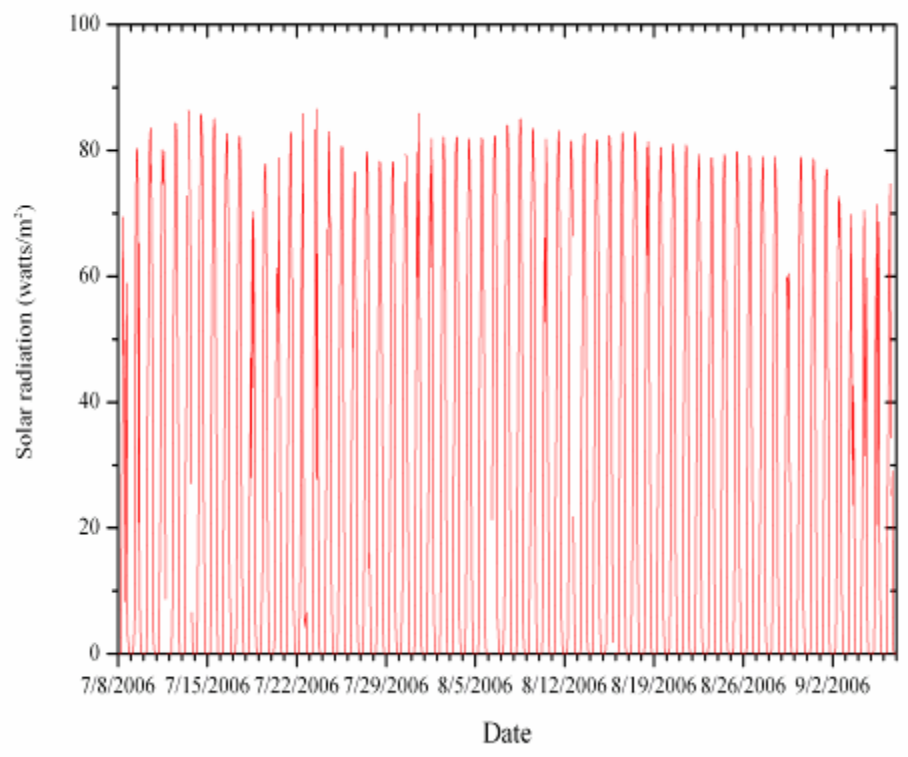

Figure 18. Solar radiation (in watts/m^2) at Site #3 (Sarcobatus Flat).

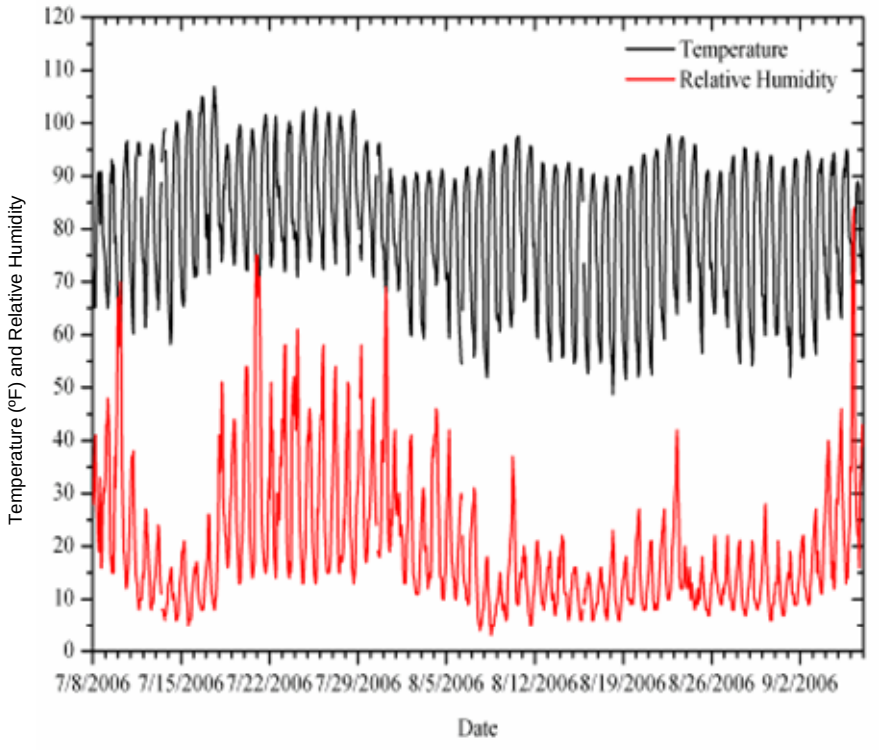

Figure 19. Temperature (in ºF) and relative humidity at Site #3 (Sarcobatus Flat).

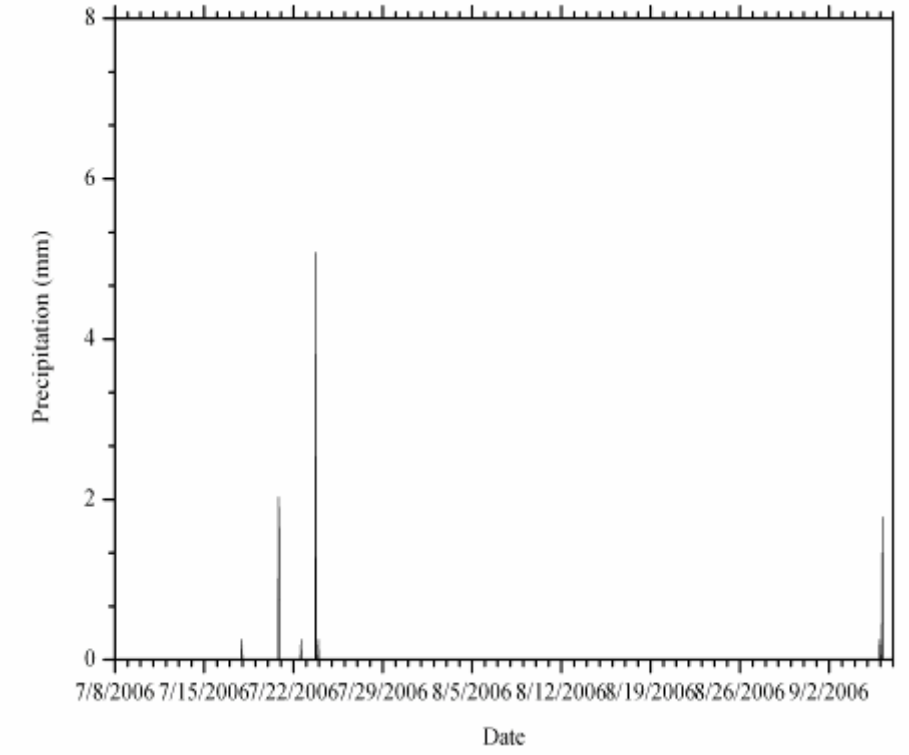

Figure 20. Total precipitation (in mm) at Site #3 (Sarcobatus Flat).

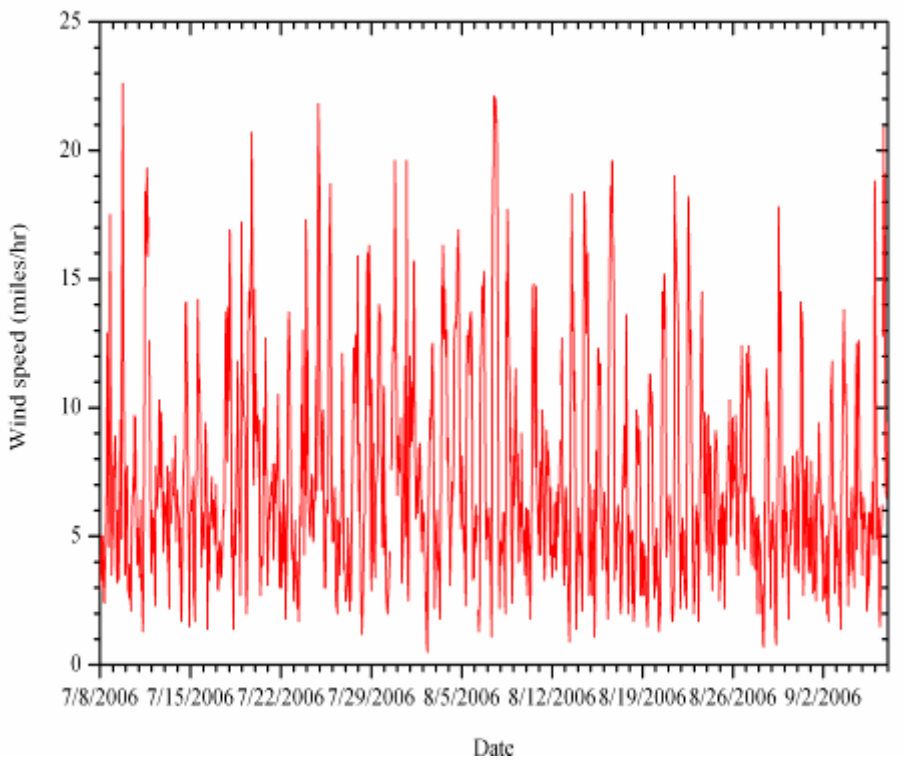

Figure 21. Wind speed (in miles/hr) at Site #3 (Sarcobatus Flat).

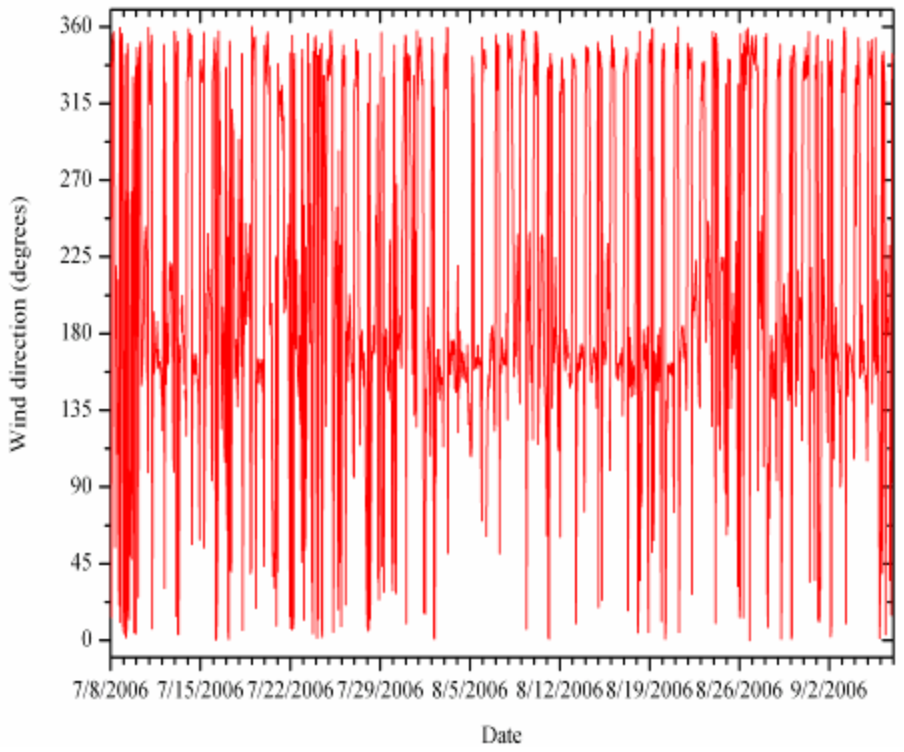

Figure 22. Wind direction at Site #3 (Sarcobatus Flat).

Wind conditions for the monitoring period were described by northwest winds during the night and southeast winds during the day with wind speeds mostly in the range of 5 to 15 miles/hour (Figure 21 and Figure 22). The classification of wind conditions was retrieved from the Federal Meteorological Handbook (Table 6). The mean wind speed for each direction bin (16 bins) is presented in Figure 23.

Table 6. Wind condition classifications.

Miles/hour	Specification
<1	Calm; smoke rises vertically.
1 to 5	Direction of wind shown by smoke drift not by wind vanes. Wind felt on face; leaves rustle; vanes moved by wind.
5 to 9	Leaves and small twigs in constant motion; wind extends light flag.
9 to 14	Raises dust, loose paper; small branches moved.
14 to 23	Small trees in leaf begin to sway; crested wavelets form on inland waters. Large branches in motion; whistling heard in overhead wires; umbrellas used with difficulty.
23 to 35	Whole trees in motion; inconvenience felt walking against wind. Breaks twigs off trees; impedes progress.
35 to 48	Slight structural damage occurs. Trees uprooted; considerable damage occurs.
>48	Widespread damage.

(retrieved from Federal Meteorological Handbook; Chapter 5. Wind; ***http://www.nws.noaa.gov/oso/oso1/oso12/fmh1/fmh1ch5.htm#chp5link***)

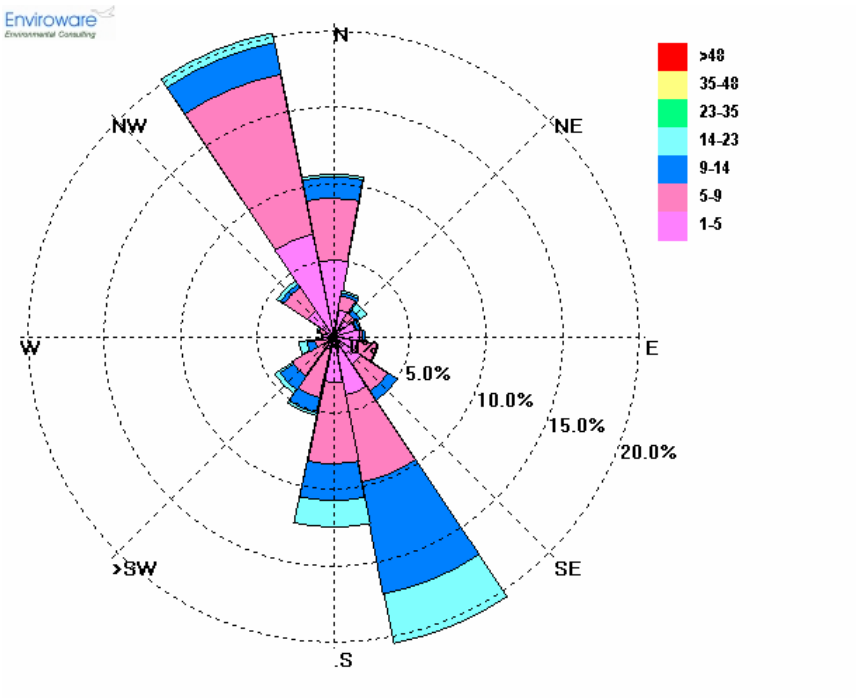

Figure 23. Wind direction and speed at Sarcobatus Flat.

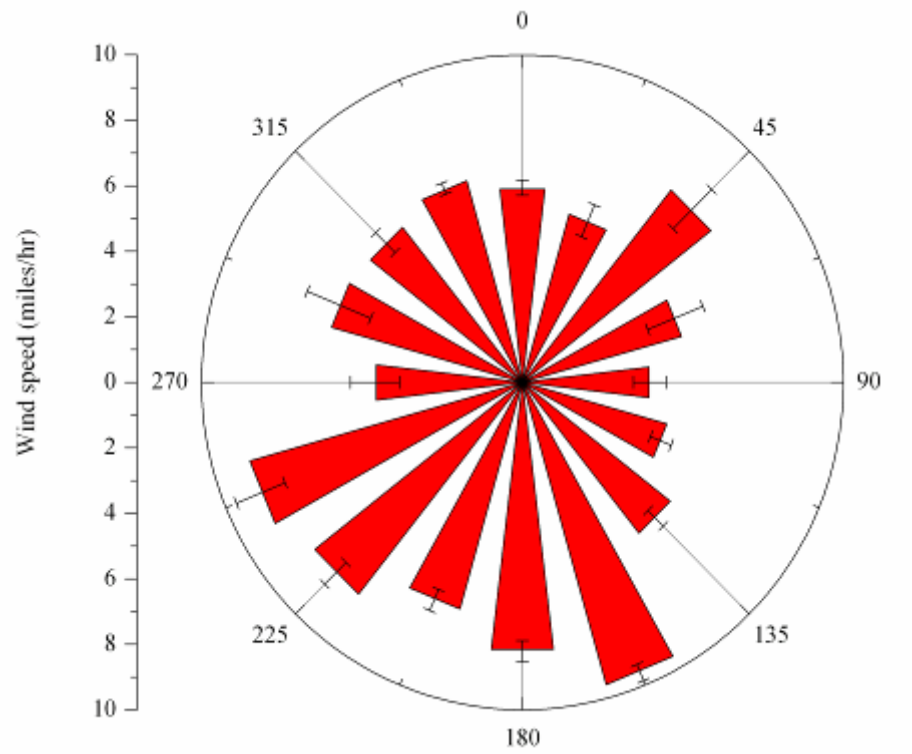

Figure 24. Average wind speed for each wind direction sector. Error bars represent the standard error of the mean.

For the entire monitoring period, winds were blowing from the northwest and southeast. Less than 3 percent of southeast winds were associated with wind speeds higher than 14 miles/hour, with a mean wind speed of 9.9 miles/hour. This is consistent with the topography of the region (Figure 2). Lower wind speeds are recorded for winds blowing from the northeast (mean wind speed of 6 miles/hour) (Figure 24).

Associations of Meteorology with Aerosol Measurements

Trends and correlations of PM mass with meteorological conditions are shown for hourly TEOM data. The increase in wind speed triggered higher PM_{10} concentrations but a gradual decrease on $PM_{2.5}$ concentrations. A rather bimodal pattern is observed for both fractions of particle mass (Figure 25). The first mode is associated with comparatively higher particle mass concentration in early morning (5:00 to 6:00) followed by a gradual decrease. A second, less pronounced, mode can be observed in late afternoon (18:00 to 20:00), especially for the fine fraction. There are no significant differences of $PM_{2.5}$ concentrations for different wind directions, while somewhat higher PM_{10} levels were determined for north/east-northeast winds as compared to those blowing from the south (Figure 26 and Figure 27).

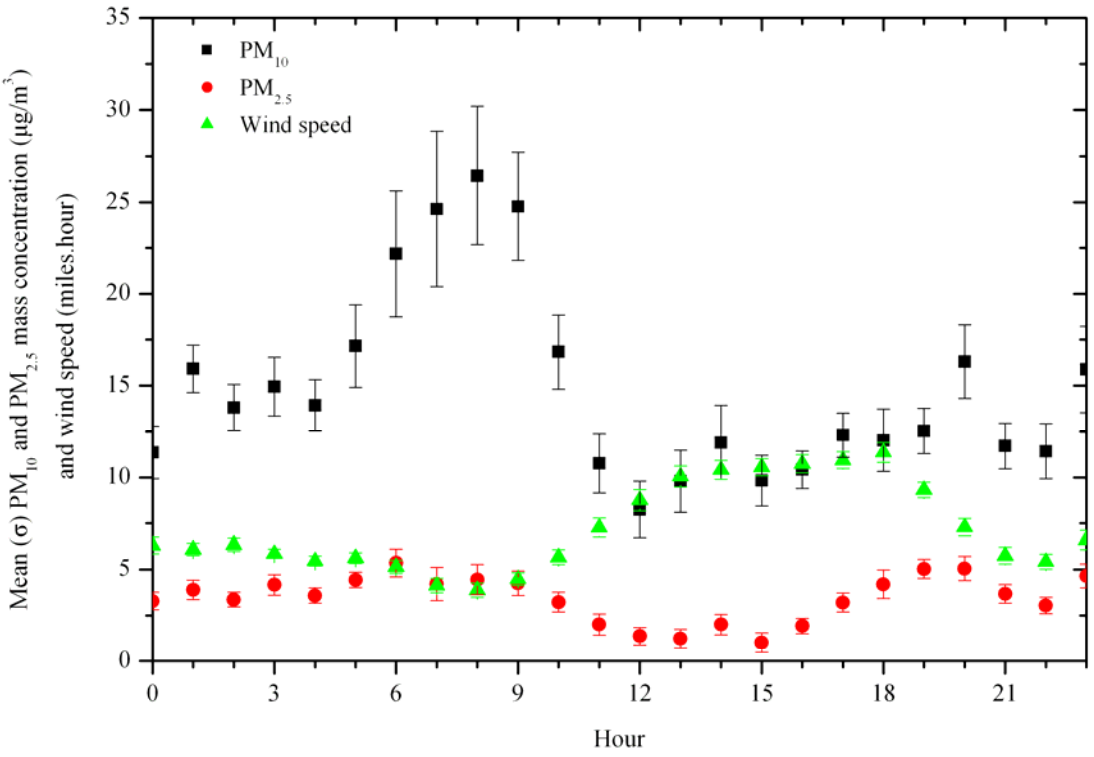

Figure 25. Hourly variation of PM_{10} and $PM_{2.5}$ mass concentrations ($\mu g/m^3$) as well as wind speed (miles/hour) at Site #3 (Sarcobatus Flat). Error bars represent the standard error of the mean.

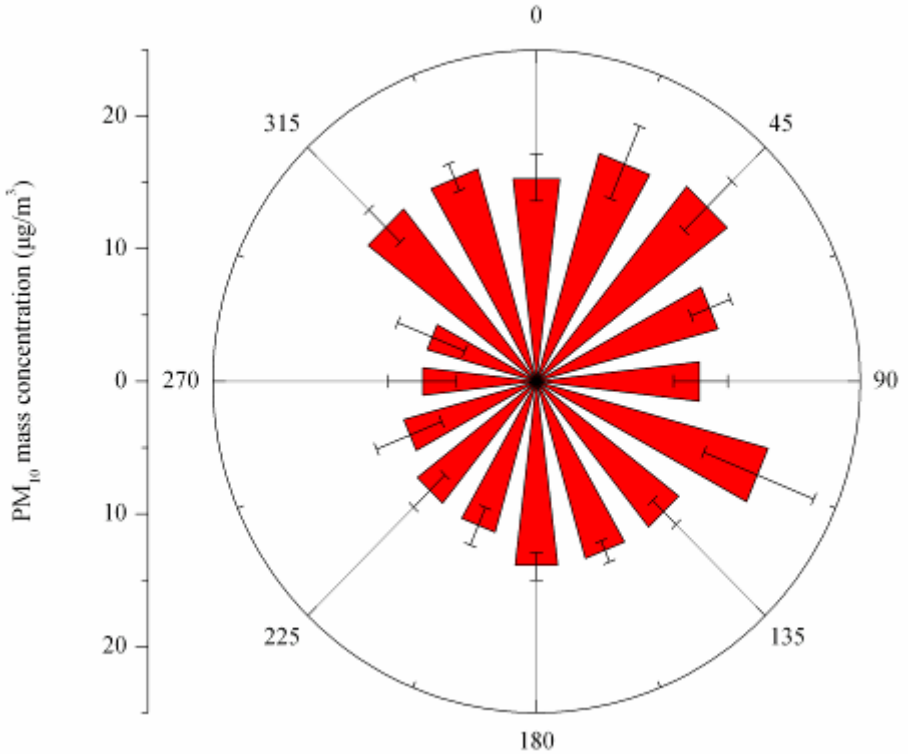

Figure 26. Mean (± st.error) of PM_{10} mass concentrations ($\mu g/m^3$) for different wind direction sectors at Site #3 (Sarcobatus Flat).

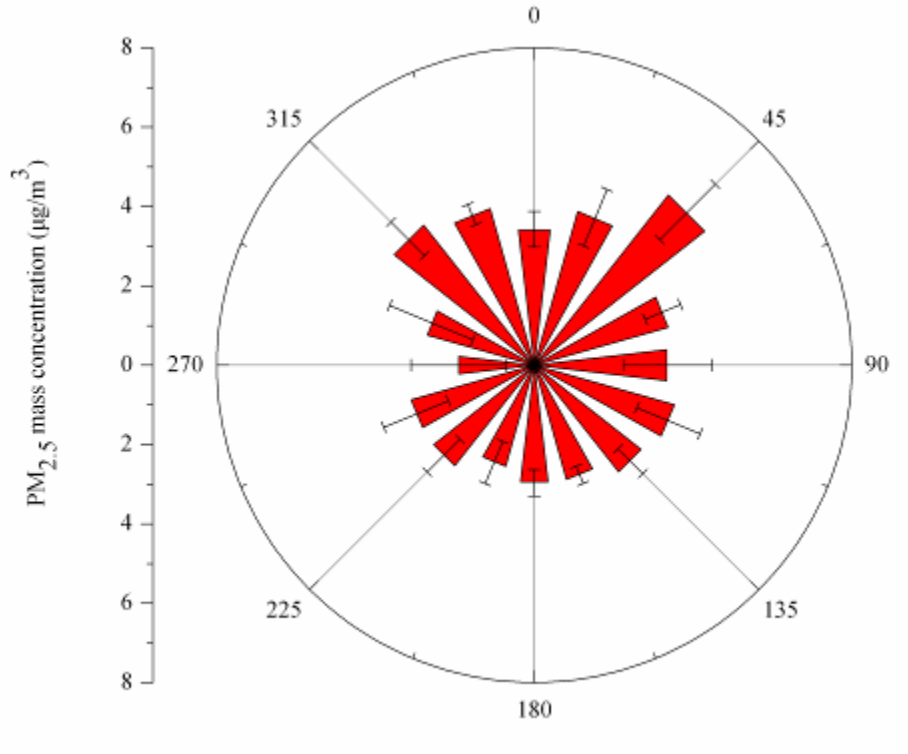

Figure 27. Mean (± st.error) of $PM_{2.5}$ mass concentrations ($\mu g/m^3$) for different wind direction sectors at Site #3 (Sarcobatus Flat).

CONCLUSIONS

PM_{10} and $PM_{2.5}$ mass concentrations and meteorological conditions were continuously monitored from July 06 to September 07, 2006, in Sarcobatus Flat, with continuous (TEOM and DUSTTRAK) monitors. At the same time, integrated samples of PM_{10} and $PM_{2.5}$ were collected using FRM samplers on a 1-to-6-day schedule. Two sets of filters (July 28 and August 15, 2006) were analyzed for major anions (sulfate, nitrate, chloride) and cations (sodium and potassium), elements (from sodium to uranium), and elemental and organic carbon. The comparison of PM_{10} and $PM_{2.5}$ mass concentrations obtained by continuous monitors and filters showed that differences are associated with the limitations of the operating principle. For example, while light scattering (the measurement technique for DUSTTRAK) is not influenced by volatilization losses and is accurate for fine particles, it performs poor for coarse particles, resulting in underestimation of PM_{10} mass. TEOM PM_{10} measurements were subject to volatilization artifacts at relatively high PM_{10} concentrations. $PM_{2.5}$ mass measurements obtained by TEOM, DUSTTRAK, and filter-based methods were comparable.

Mean 24-h concentrations of PM_{10} and $PM_{2.5}$ mass were 14.8 and 3.5 $\mu g/m^3$, which are significantly lower than the 24-h and annual NAAQS standards (24-h PM_{10}: 150 $\mu g/m^3$, 24-h $PM_{2.5}$: 35 $\mu g/m^3$; Annual $PM_{2.5}$: 15 $\mu g/m^3$). Higher PM_{10} and $PM_{2.5}$ mass concentrations in the early morning and late afternoon indicated the contribution of traffic emissions from U.S. Highway 95. Comparatively lower PM_{10} and $PM_{2.5}$ levels were associated with increased wind speeds blowing mostly from the north/northwest in early afternoon. The

chemical composition of both PM_{10} and $PM_{2.5}$ samples indicated that organic carbon is the major component of both fractions, while soil contributes approximately 50 percent of PM_{10} mass. Sulfate and nitrate account for about 10 percent. Increases in PM_{10} and $PM_{2.5}$ mass concentrations are associated with higher concentrations of organic mass. However, the importance of organic carbon mass may be overestimated, especially for fine particles, because of the absorption of low-vapor pressure organic gases by the quartz filter.

ACKNOWLEDGEMENTS

Authors thank Mrs. Joan Terrell for hosting the mobile trailer on her property.

REFERENCES

Kavouras, I.G., V. Etyemezian, D. DuBois, J. Xu, M. Pitchford, and M. Green. 2005. Assessment of the Principal Causes of Dust-Resultant Haze at IMPROVE Sites in the Western United States. Final report to Western Regional Air Partnership (www.coha.dri.edu/dust).

Lefer, B.L. and R.W. Talbot. 2001. Summertime measurements of aerosol nitrate and ammonium at a northeastern U.S. site. *Journal of Geophysical Research,* 106, 20,365 – 20,378.

Malm, W.C., B.A. Schichtel, R.B. Ames, and K.A. Gebhart. 2002. A 10-year spatial and temporal trend of sulfate across the United States. *Journal of Geophysical Research,* 107, 4627, doi:10.1029/2002JD002107

Malm, W.C., B.A. Schichtel, M.L. Pitchford, L.L. Ashbaugh, and R.A. Eldred. 2004. Spatial and monthly trends in speciated fine particle concentration in United States. *Journal of Geophysical Research*, 109, D03306, doi:10.1029/2006JD003739.

White, W.H. and P.T. Roderts. 1977. On the nature and origins of visibility-reducing aerosol in the Los Angeles air basin. *Atmospheric Environment*, 11, 803-812.